Science Advances

AAAS

advances.sciencemag.org/cgi/content/full/2/6/e1600148/DC1

Supplementary Materials for

Oil droplet self-transportation on oleophobic surfaces

Juan Li, Qi Hang Qin, Ali Shah, Robin H. A. Ras, Xuelin Tian, Ville Jokinen

Published 17 June 2016, *Sci. Adv.* **2**, e1600148 (2016)
DOI: 10.1126/sciadv.1600148

This PDF file includes:

Other Supplementary Material for this manuscript includes the following:
(available at advances.sciencemag.org/cgi/content/full/2/6/e1600148/DC1)

- movie S1 (.mov format). Demonstration of three modes of oil droplet motion on various sample surfaces.
- movie S2 (.mov format). Self-transportation of ethanol-water mixture droplets with different compositions on sample B3.
- movie S3 (.mov format). Self-transportation of an ethanol droplet on sample A5.

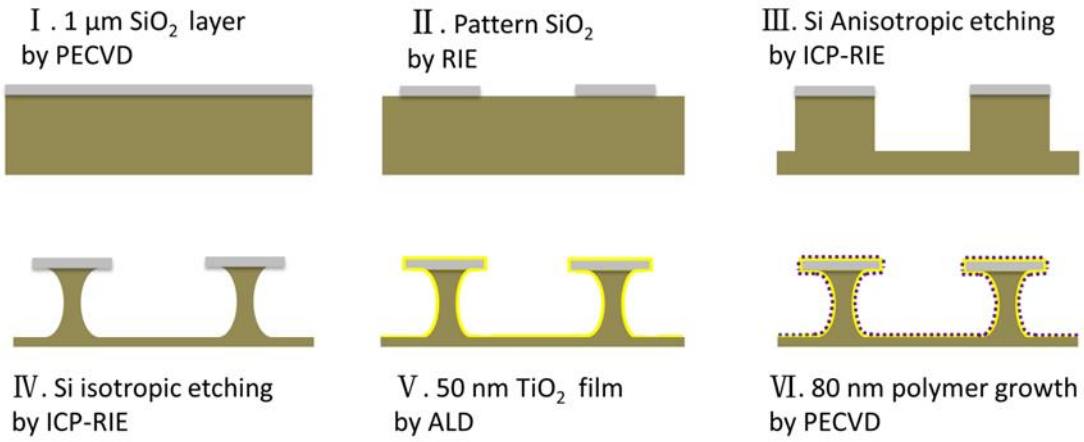

fig. S1. Fabrication process flow for the radial undercut patterns with TiO_2 and polymer coatings.

Ⅰ. Plasma enhanced chemical vapor deposition (PECVD) for 1 μm SiO_2 layer
Oxford Instruments, Plasmalab 80 Plus, T = 300 °C, Pressure = 1000 mTorr, Power = 20 W, Process Gas: SiH_4 = 8.4 sccm. The deposition time for 1 μm SiO_2 layer was 15 min.

Ⅱ. Photolithography and reactive ion etching (RIE) for SiO_2 Patterns
Oxford Instruments, Plasmalab 80Plus, Pressure = 30 mTorr, Forward power = 200 W, CHF_3 = 25 sccm, Ar = 25.0 sccm. The etching time for 1 μm SiO_2 was 30 min.

Ⅲ. ICP-RIE for Si anisotropic etching
Oxford Instruments: Plasmalab System100 - ICP 180. ICP-Forward power 1050 W, SF_6: 40sccm/ O_2: 6 sccm. Pressure: 8 mTorr, T = -110°C. The anisotropic Si etching rate was 2 μm/min.

Ⅵ. ICP-RIE for Si isotropic etching
Oxford Instruments: Plasmalab System100 - ICP 180. ICP-Forward power 500 W, SF_6: 50 sccm, set pressure: 30 mTorr, T = -100°C. The isotropic etching time for 1.2 μm undercut was 6 min.

Ⅴ. Atomic layer deposition (ALD) for 50 nm TiO_2
Beneq, TFS-500, temperature 300°C, rate: 0.0426 nm/cycle, precursors: $TiCl_4$ and H_2O.

Ⅵ. PECVD for 80 nm fluoropolymer
Oxford Instruments, Plasmalab 80 Plus, rate: 8 nm/min, CHF_3 100 sccm, pressure 250 mTorr, forward power: 50 W.

table S1. Geometrical parameters of different patterns and their contact angles, wettability gradients, and breakthrough pressure equations.

Samples	D (μm)	Φ (°)	1. θ (°) 2. $-d(cos\theta)/dL$ (mm^{-1}) 3. P_c (Pa) $Test\ liquid: Hexadecane, \theta_0 = 55°, \gamma = 27.5\ mN/m$
A1	7.0	5	$\theta = arccos(0.13/L - 1)$ $-dcos\theta/dL = 0.13/L\text{^}2$ $P_c = 44.608/(L \times 0.0872 - 0.007)$
A2	7.0	2.5	$\theta = arccos(0.26/L - 1)$ $-dcos\theta/dL = 0.26/L\text{^}2$ $P_c = 44.608/(L \times 0.0436 - 0.007)$
A3	7.0	1.25	$\theta = arccos(0.53/L - 1)$ $-dcos\theta/dL = 0.53/L\text{^}2$ $P_c = 44.608/(L \times 0.0218 - 0.007)$
A4	7.0	0.625	$\theta = arccos(1.06/L - 1)$ $-dcos\theta/dL = 1.06/L\text{^}2$ $P_c = 44.608/(L \times 0.0109 - 0.007)$
A5	7.0	0.3125	$\theta = arccos(2.10/L - 1)$ $-dcos\theta/dL = 2.10/L\text{^}2$ $P_c = 44.608/(L \times 0.0055 - 0.007)$
B1	12.0	5	$\theta = arccos(0.23/L - 1)$ $-dcos\theta/dL = 0.23/L\text{^}2$ $P_c = 44.608/(L \times 0.0872 - 0.012)$
B2	12.0	2.5	$\theta = arccos(0.45/L - 1)$ $-dcos\theta/dL = 0.45/L\text{^}2$ $P_c = 44.608/(L \times 0.0436 - 0.012)$
B3	12.0	1.25	$\theta = \arccos(0.89/L - 1)$ $-dcos\theta/dL = 0.89/L\text{^}2$ $P_c = 44.608/(L \times 0.0218 - 0.012)$
B4	12.0	0.625	$\theta = \arccos(1.78/L - 1)$ $-dcos\theta/dL = 1.78/L\text{^}2$ $P_c = 44.608/(L \times 0.0109 - 0.012)$
C1	17.0	5	$\theta = arccos(0.31/L - 1)$ $-dcos\theta/dL = 0.31/L\text{^}2$ $P_c = 44.608/(L \times 0.0872 - 0.017)$
C2	17.0	2.5	$\theta = arccos(0.63/L - 1)$ $-dcos\theta/dL = 0.63/L\text{^}2$ $P_c = 44.608/(L \times 0.0436 - 0.017)$
C3	17.0	1.25	$\theta = arccos(1.25/L - 1)$ $-dcos\theta/dL = 1.25/L\text{^}2$ $P_c = 44.608/(L \times 0.0218 - 0.017)$

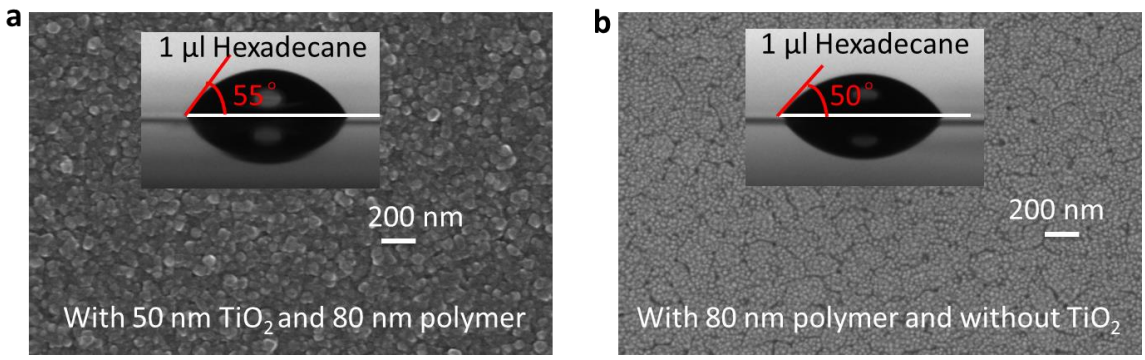

fig. S2. SEM images and contact angles of TiO_2 and fluoropolymer-coated surfaces and merely fluoropolymer-coated surfaces. (**a**) Flat surface with TiO_2 layer and fluoropolymer coating, showing a contact angle of ~ 55° to a hexadecane droplet. (**b**) Flat surface only with fluoropolymer layer, showing a contact angle of ~ 50° to hexadecane. The TiO_2 coating thus improves θ_0 and can enhance the robustness of the solid-air composite interface to support oil droplets on the patterned surfaces.

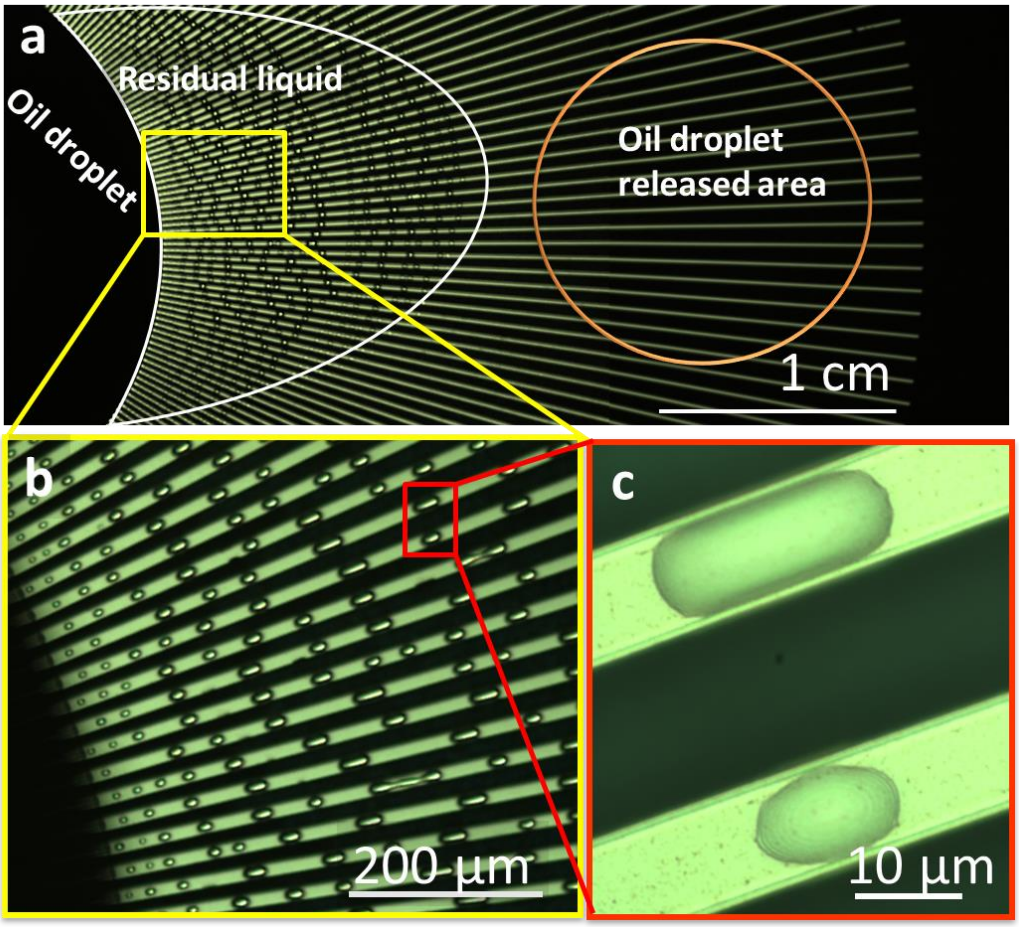

fig. S3. Residual hexadecane left on pattern B3 after droplet self-transport. (**a**) Optical microscopic image showing residual hexadecane micro-droplets close to the pattern center (in the area enclosed by the white line). The left black area is the transported droplet on the pattern center, and the orange circle indicates the position where the droplet was released. (**b-c**) Enlarged images showing the residual micro-droplets.

The formation of residual micro-droplets is similar to what was observed on superomniphobic surfaces after droplet sliding or evaporation due to liquid bridge pinch-off caused by contact line receding through discrete posts (*27*). For our patterns, though liquid bridge pinch-off is not likely to happen when the contact line recedes radially along the stripes, it could happen when the contact line recedes laterally (i.e. through different stripes). At the early stage of droplet self-transport, the contact line advances laterally due to the increasing contact base caused by inward wettability gradient, and is not able to induce pinching off; only at the later stage when the droplet begins to enter into the center area, the contact line starts to recede laterally, which then induces liquid bridge pinching off and leads to residual liquid on top of the stripes. This is why the residual liquid is only observed nearby the pattern center. Moreover, the residual liquid on the very thin and relatively hydrophobic individual stipes could not exist in film form and would break into tiny droplets to reduce the surface energy, as observed above. The total volume of the residual micro-droplets is estimated to be only on the order of 0.01% of that of the original droplet.

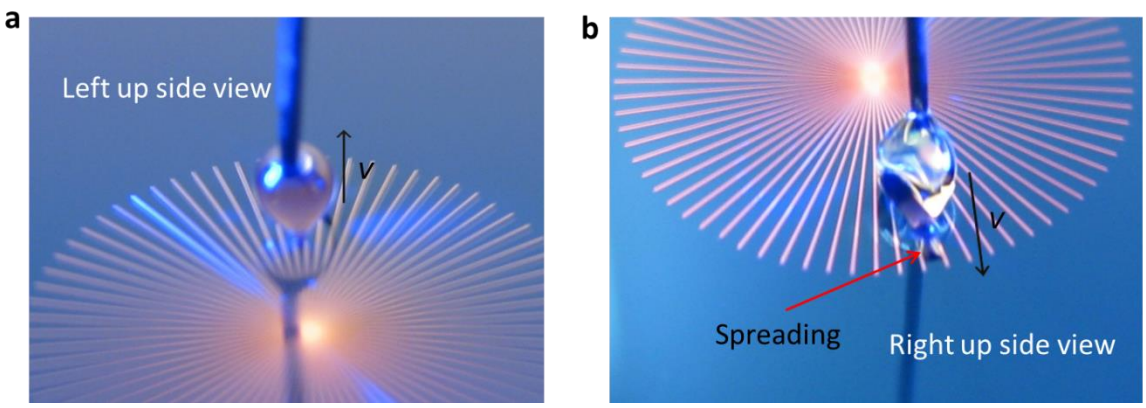

fig. S4. The outward spreading of an oil droplet of 1 µl on the A1 pattern. (**a**) No spreading oil film was seen at the front of the droplet. (**b**) Spreading oil film was seen at the back side of the droplet.

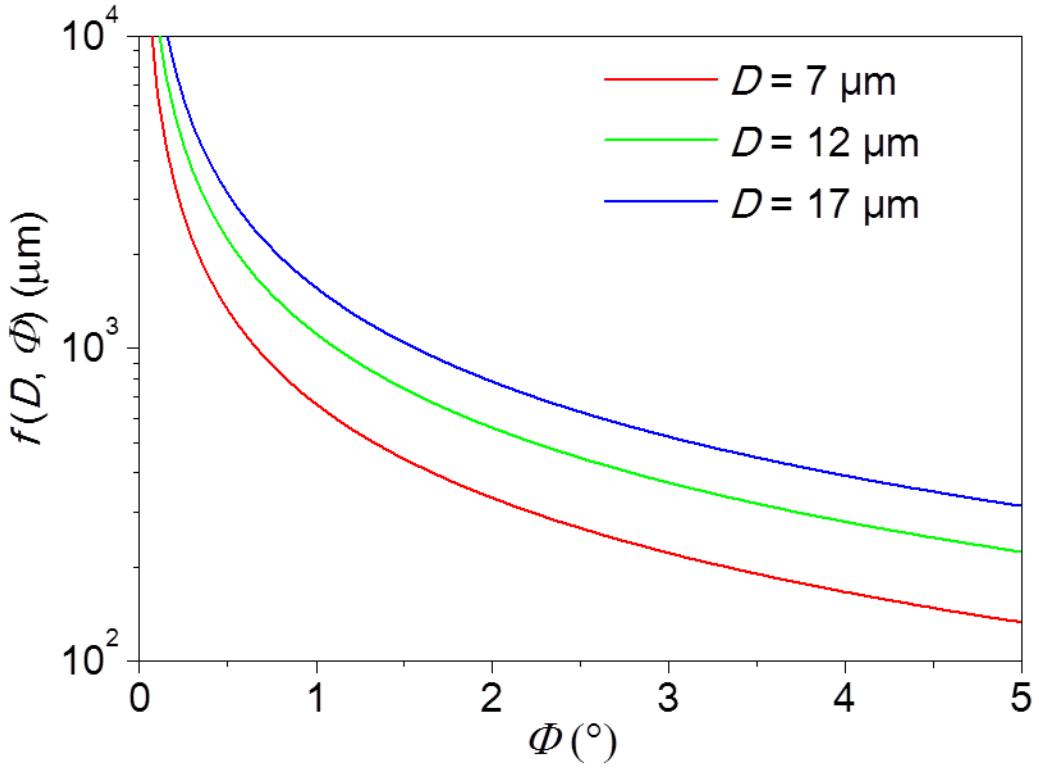

fig. S5. The effect of *D* and Φ on the driving force for droplet motion.

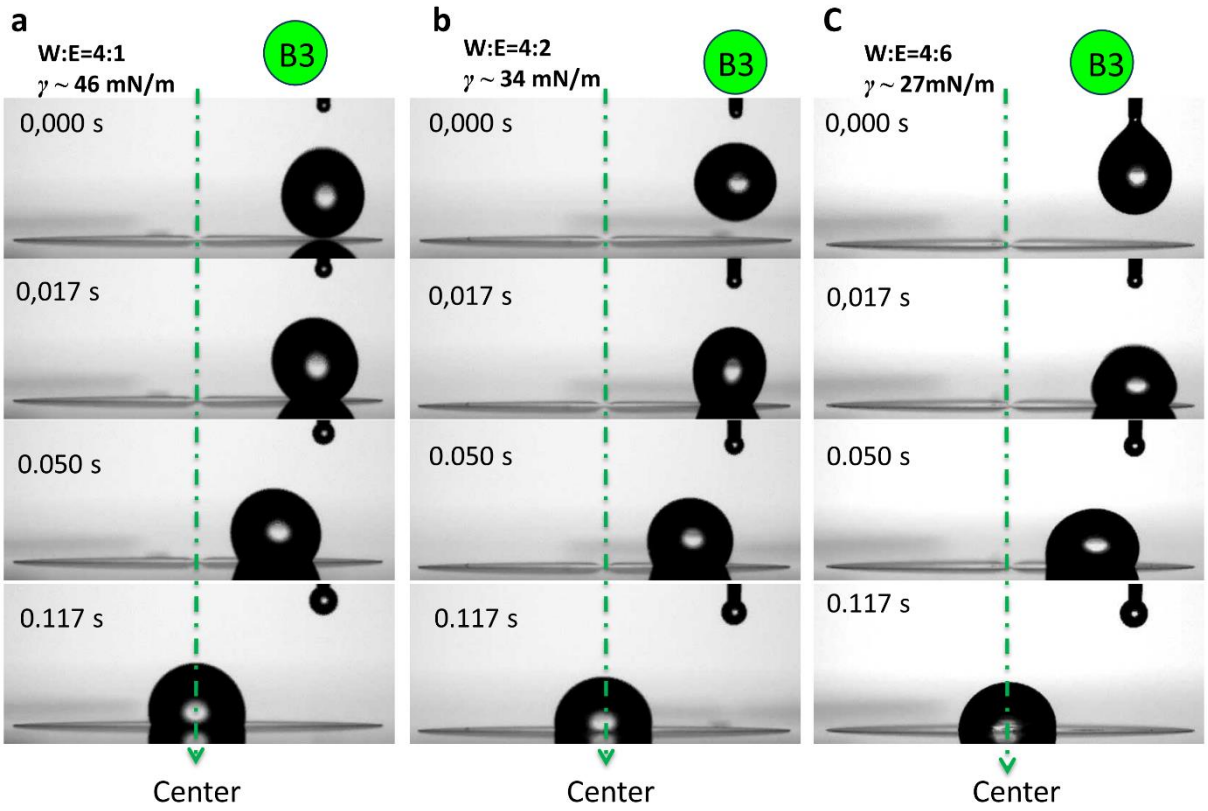

fig. S6. **Self-transportation of water-ethanol mixture droplets of different compositions on sample B3.** (**a**) water : ethanol (v/v) = 4 : 1. (**b**) water : ethanol (v/v) = 4 : 2. (**c**) water : ethanol (v/v) = 4 : 6.

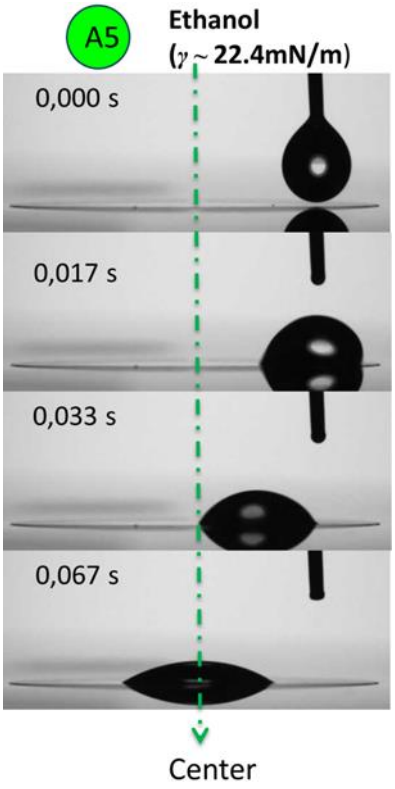

fig. S7. Self-transportation of an ethanol droplet on sample A5.

table S2. **Effect of pattern parameters on self-transport speed of hexadecane droplets.**

Pattern number	Velocity (cm/s)
A5	2.98
B4	2.75
C3	2.68
A4	2.60
B3	2.40

*Droplet volume was 3 μL, which was released ~3 cm away from the pattern center.

As shown above, the self-transport speed (V) of hexadecane droplets varies from 2.98 cm/s to 2.40 cm/s on the five patterns that belong to the green group, obeying the following trend: $V_{A5} > V_{B4} > V_{C3} > V_{A4} > V_{B3}$. This trend is in well accordance with the wettability gradient of the samples (Fig. 4B), that is, the pattern with larger wettability gradient shows larger droplet speed.

table S3. Effect of liquid type on self-transport speed of droplets.

Liquid	Velocity (cm/s)
water-ethanol (v:v = 4:1)	2.40
water-ethanol (v:v = 4:2)	2.56
water-ethanol (v:v = 4:6)	2.68
hexadecane	2.60

*Pattern A4 was used, and droplet volume was 3 μL, which was released ~3 cm away from the pattern center.

In contrast to pattern parameters, the effect of liquid type is less pronounced. The speed shows slight increase with decreased liquid surface tension, for example, from 2.40 cm/s for water-ethanol mixture droplets (v : v = 4:1, γ ~ 46 mN/m) to 2.68 cm/s (v : v = 4 : 6, γ ~ 27 mN/m), attributed to the increased droplet contact radius. Meanwhile, liquid with high viscosity showed slower speed due to increased viscous dissipation, as evidenced by hexadecane, which has a similar surface tension to water-ethanol (v : v = 4 : 6) but a higher viscosity, exhibited a lower speed of 2.60 cm/s.

movie S1. Demonstration of three modes of oil droplet motion on various sample surfaces. Left: inward oil droplet self-transportation; middle: pinned droplet; right: outward droplet spreading.

movie S2. Self-transportation of ethanol-water mixture droplets with different compositions on sample B3.

movie S3. Self-transportation of an ethanol droplet on sample A5.